

# Aluminum-silicon coatings on austenitic stainless steel (AISI 304 and 317) deposited by chemical vapor deposition in a fluidized bed

## Recubrimientos de aluminio-silicio sobre acero inoxidable austenítico AISI 304 Y 317 por deposición química de vapor en lecho fluidizado

J. L. Marulanda Arevalo<sup>1</sup>, F. J. Pérez Trujillo<sup>2</sup> and S. I. Castañeda<sup>3</sup>

### ABSTRACT

Aluminum-silicon coatings were deposited onto stainless steels AISI 304 and AISI 317. The deposition was performed at 540°C with a ratio of active gases HCl/H<sub>2</sub> of 1/15.3; argon was used as a carrier gas. The bed of the FBR-CVD process consisted of 2.5 g aluminum powder, 7.5 g silicon powder and 90 g alumina. After the coatings were deposited, each sample was given a heat treatment to improve its mechanical properties and oxidation behavior by diffusing the alloying elements. Thermodynamic simulation was performed with Thermo-Calc software to investigate the composition of the deposited material. The coated and uncoated specimens were exposed to temperatures of 750 °C in an atmosphere where the vapor was transported to the samples using a flow of N<sub>2</sub> of 40 ml/min and 100% water vapor (H<sub>2</sub>O). The coated specimens gained little weight during the thousand hours of exposure and will thus guard against a corrosive attack compared to the uncoated substrates. In addition, the coated stainless steels show an oxidation rate with a logarithmic trend while the uncoated steel oxidation rate showed a linear trend.

**Keywords:** Coating, aluminum-silicon, chemical vapor deposition, high temperature oxidation, stainless steel, oxidation rate, steam oxidation.

### RESUMEN

Se obtuvieron recubrimientos de aluminio-silicio en los aceros inoxidables AISI 304 y AISI 317. La deposición se realizó a 540 °C, con una proporción de gases activos (HCl/H<sub>2</sub>: 1/15.3), como gas de arrastre se utilizó argón. El lecho del proceso CVD-FBR estaba formado por 2,5 g de polvo de aluminio, 7,5 g polvo de silicio y 90 g de alúmina. Después de depositados los recubrimientos, se le dio un tratamiento térmico para mejorar sus propiedades mecánicas y su comportamiento frente a la oxidación, por entre la difusión de los elementos de aleación. La simulación termodinámica se realizó con el software Thermo-Calc para obtener información sobre la posible composición del material depositado. Las muestras recubiertas y sin recubrir, se expusieron a 750 °C en una atmósfera donde el vapor se transporta a las muestras usando un flujo de N<sub>2</sub> de 40 ml / min y 100% de vapor de agua (H<sub>2</sub>O). Aceros recubiertos ganaron algo de peso durante las mil horas de exposición y resisten muy bien el ataque corrosivo frente a los sustratos recubiertos. Además, los aceros inoxidables recubiertos muestran una velocidad de oxidación con tendencia logarítmica, mientras que la velocidad de oxidación de acero sin recubrimiento tiene tendencia lineal.

**Palabras clave:** Recubrimiento, Aluminio/Silicio, Deposición Química de Vapor, Oxidación a Alta temperatura, acero inoxidable, velocidad de oxidación, oxidación en vapor.

Received: December 17th 2013

Accepted: May 5th 2014

### Introduction

The need to protect surface components that operate at high temperatures has increased significantly. Coatings are an effective method to improve the surface properties of materials. Additionally, reactive metals in the coatings diffuse into the substrate to a considerable depth; essentially, diffusion layers work as the alloy

surface with a gradient of composition with a small amount of an expensive super alloy on the surface (Christoglou, Voudoris, & Angelopoulos, 2002; Anastassiou, Christoglou, & Angelopoulos, 2010; Hao-Tung, Sheng-Chang, Jow-Lay, & Shin-Yun, 2007). Increasing the temperature capabilities of a material for advanced power generation applications is of great importance due to the

<sup>1</sup> Jose Luddey Marulanda Arevalo. Doctor en Química Avanzada, Universidad Complutense de Madrid, Spain. Affiliation: Profesor asociado, Universidad Tecnológica de Pereira (UTP), Colombia. E-Mail: jlmraulanda@utp.edu.co

<sup>2</sup> Francisco Javier Pérez Trujillo. Doctor, Universidad Complutense de Madrid (UCM), Spain. Affiliation: Profesor, Universidad Complutense de Madrid (UCM). Grupo de investigación en Ingeniería de Superficies y Materiales Nano estructurados, Spain. E-Mail: fjperez@quim.ucm.es.

<sup>3</sup> Saul Isaac Castañeda. Doctor, Universidad Complutense de Madrid (UCM). Affiliation: Investigador, Universidad Complutense de Madrid (UCM). Grupo de investigación en Ingeniería de Superficies y Materiales Nano estructurados, Spain. E-Mail: sicastan@quim.ucm.es.

**How to cite:** Marulanda, J. L., Pérez, F. J., & Castañeda, S. I. (2014). Aluminum-silicon coatings on austenitic stainless steel (AISI 304 and 317) deposited by chemical vapor deposition in a fluidized bed. *Ingeniería e Investigación*, 34(2), 5-10.

potential gain in energy efficiency and the decrease in pollutant emissions (Perez et al., 2006a). Chemical vapor deposition is a versatile process that allows the application of different metal and ceramic materials for the protection of materials against wear, corrosion and oxidation at high temperatures in the aircraft industry, military and engineering in general. The process of chemical vapor deposition is a dynamic and complex system, where the thermodynamics, kinetics and transport phenomena are essential steps that utilize the chemical reactions of precursor gases to form a solid and stable product (Choy, 2003; Abella, 2003; Brossard, Hierro, Sanchez, Bolivar, & Pérez, 2006). Chemical vapor deposition in a fluidized bed (CVD-FBR) is a variant of the chemical vapor deposition process. The CVD-FBR combines the advantages of thermal activation by heating and the fluidized bed, which provides the high mass and thermal transfer between the gas, the bed and the samples inside the reactor. The samples were placed above the fluidized bed, which produced a more uniform temperature and good mixing of the reactive gases with the fluidized particles, achieving a high degree of reaction of all species activated in the bed. As a result, there is excellent contact between the solid particles and the fluidization gas (Perez, Pedraza, Hierro, & Hou, 2000; Zhan, He, Wang, & Gao, 2006; D. Chaliampalias, Vourlias, Pistofidis, Pavlidou, & Stergiou, 2007). The main disadvantage of CVD-FBR is the need for a well-designed gas distributor, which is inevitably associated with the gradual deposition of solids and the generation of agglomerates due to the frequency of relative motion. The proper design of the reactor geometry ensures efficient contact between the gas and solid, as well as uniformity in the movement of the solid, which is very important for obtaining quality coatings (Perez et al., 2006a; Tsipas, Anthimides, & Flitris, 2003; Golman, & Shinohara, 1999; Kim, & Young, 2006).

The determination of the process conditions (i.e., temperature, reactant concentration and gas flow rate) is always a critical step in the deposition of coatings. In all cases, a thermodynamic study of the phase equilibrium (i.e., composition and partial pressure) during the CVD process is necessary to determine the feasibility of the metal deposition and provides a useful guideline to improve the deposition condition (Brossard, Hierro, Sanchez, Bolivar, & Pérez, 2006).

The use of aluminum layers is an effective way to increase the corrosion resistance of steels. This protection is obtained by forming a surface film of  $\text{Al}_2\text{O}_3$ . The coating grows by internal diffusion of the aluminum, as the iron and chromium diffuse outward (Christoglou, Voudouris, Angelopoulos, Pant, & Danhl, 2004). The inherent property of aluminum to form stable layers of  $\text{Al}_2\text{O}_3$  in atmospheres containing oxygen is well known and has been adapted for the surface enrichment of steel components that operate in aggressive environments at high temperature because alumina has excellent mechanical properties and good chemical stability at high temperatures (Sanchez, Bolivar, Hierro, & Pérez, 2008).

## Experimental procedure

Specimens of the austenitic stainless steels AISI 304 and AISI 317 with dimensions 20 mm x 6 mm x 2 mm were used. For this study of aluminum-silicon co-deposition, the specimens were machined and polished using emery paper No. 100 to No. 600 and then cleaned in an ultrasonic bath of ketones for 10 minutes. Thermodynamic simulations were performed to investigate the optimum conditions for the co-deposition of aluminum-silicon coatings with CVD-FBR using Thermo-Calc software (ThermoCalc Software, 2003). The calculations are based on the free Gibbs energy minimization method and mass conversion rule. The thermodynamic simulation was performed with Thermo-Calc software, combining

the SSOL2 and SSUB3 databases of the Scientific Group Thermo-data Europe to define the gaseous species and solid species. These calculations were performed to determine the effects of the main CVD-FBR parameters (i.e., T, gas composition and powder mixture) on the equilibrium partial pressure of the generated Al-Si precursors. The main gas precursors and phases formed at equilibrium in the temperature range of 460 - 640 °C were investigated and provide an understanding of the reactions occurring during deposition. The schematic diagram of the CVD-FBR system used in this study is described elsewhere (Perez et al., 2006b). The reactor was made of a quartz tube and was heated by an external furnace. The bed used was composed of a mix of aluminum powder of 99.5 % of purity and 400  $\mu\text{m}$  particle size, and silicon powder of 99.5 % of purity and 200  $\mu\text{m}$  particle size as the donor; 90 wt% alumina ( $\text{Al}_2\text{O}_3$ ) was used as the inert bed. The powder mixture was fluidized by Ar gas (99.999 % purity), and hydrogen chloride plus hydrogen ( $\text{HCl} + \text{H}_2$ ) was used as an activator to generate an aluminum and silicon precursor. Mass flow meters were used for controlling the flow of  $\text{H}_2$ ,  $\text{HCl}$  and Ar. The chamber reaction temperature was controlled by a thermocouple in the fluidized bed, and the samples were suspended above the fluidized bed for the aluminum-silicon co-deposition. The coatings were deposited at temperatures below 580 °C by CVD-FBR, using the bed described. This bed was fluidized with Ar between 500 and 800 ml/min, and a mixture of  $\text{HCl}/\text{H}_2$  at a ratio of 1/12 to 1/20 was used as an activator. These tests were performed between 520 and 580 °C with exposure times of 45 minutes to 1.5 hours on the different types of austenitic stainless steels. After deposition of the CVD-FBR coatings, a diffusion heat treatment was performed in an argon gas flow at 750 °C for 2 h, followed by cooling in a furnace under an atmosphere of Ar gas. The morphology of the aluminum-silicon layers was carried out using metallographic preparation followed by a scanning electron microscope (SEM-JEOL JM-6400); the composition was studied by energy dispersed X-ray spectroscopy (EDAX), and its structure was studied by an X-ray diffractometer (XRD-PHILIPS X (PERT MPD)) through the modes  $\theta$ - $2\theta$  at a grazing angle. The specimens were exposed to 750 °C in an atmosphere where the vapor was transported to the samples by a flow of  $\text{N}_2$  at 4 ml/min with 100 % water vapor ( $\text{H}_2\text{O}$ ). The test was conducted for up to 1000 hours, taking samples at 200, 400, 600, 800 and 1000 hours. After each exposure the samples were cooled inside the furnace and the samples were weighed on an analytical balance with a precision of  $10^{-5}$  g.

## Results and discussion

### Aluminum-Silicon coatings

The results from the thermodynamic simulations were used as a guide to select the starting conditions of the FBCVD tests; information about the precursors and compounds that were formed can be determined theoretically, including the partial pressures of the main gaseous halides. The main precursors found are in agreement with those found in the literature. The thermodynamic simulation is a good tool to understand that the precursors can be formed when argon,  $\text{HCl}$  and  $\text{H}_2$  are passed through a bed containing aluminum and silicon and to help select the proportions of these gases to produce a good coating. For the thermodynamic prediction of the gas precursors, the input conditions included  $\text{Al}(\text{s})$ ,  $\text{Si}(\text{s})$  and  $\text{Ar}/\text{HCl}/\text{H}_2$  gas mixture;  $\text{Al}_2\text{O}_3$  was excluded because it is inert in the temperature range studied. This simulation was carried out between 460 and 640 °C to investigate the main precursors formed, as shown in Figure 1a, where the precursors of aluminum and silicon are formed as  $\text{AlCl}_3$ ,  $\text{Al}_2\text{Cl}_6$ ,  $\text{AlCl}_2\text{H}$ ,  $\text{ClH}_3\text{Si}$ , and  $\text{AlCl}$  and in smaller proportions as  $\text{AlCl}_2$  and  $\text{AlClH}_2$ .

The  $\text{AlCl}_3$  was the aluminum precursor that was most prevalent but was very stable; its contribution to the deposition of the aluminum layer was thus very low. The amount of  $\text{Al}_2\text{Cl}_6$  decreases with increasing temperature and drops below the amount of  $\text{AlCl}_2\text{H}$  above  $565^\circ\text{C}$ .  $\text{ClH}_3\text{Si}$  is the main precursor to deposit silicon in the coating and has a slight tendency to decrease with temperature; above  $570^\circ\text{C}$ , its amount reduces below that of  $\text{AlCl}$ . Halides react more readily and will have a greater contribution to the deposition of aluminum atoms; these include  $\text{AlCl}$ ,  $\text{AlClH}_2$ ,  $\text{AlCl}_2$  and  $\text{AlCl}_2\text{H}$ . The  $\text{AlCl}_2\text{H}$  and  $\text{AlCl}$  species are most important in the deposition of aluminum in the coating; these two species also have the highest partial pressures in the range of temperatures that were investigated. Therefore, the main species affecting deposition are  $\text{ClH}_3\text{Si}$  for the silicon deposition and the  $\text{AlCl}_2\text{H}$  and  $\text{AlCl}$  for the aluminum deposition. The amount of  $\text{ClH}_3\text{Si}$  was slightly below that of  $\text{AlCl}_2\text{H}$  and above that of  $\text{AlCl}$  up to  $570^\circ\text{C}$ , which ensures a co-deposit of Al and Si below this temperature; however, the Gibbs free energy was less negative for  $\text{ClH}_3\text{Si}$  than for  $\text{AlCl}_2\text{H}$  and  $\text{AlCl}$ .

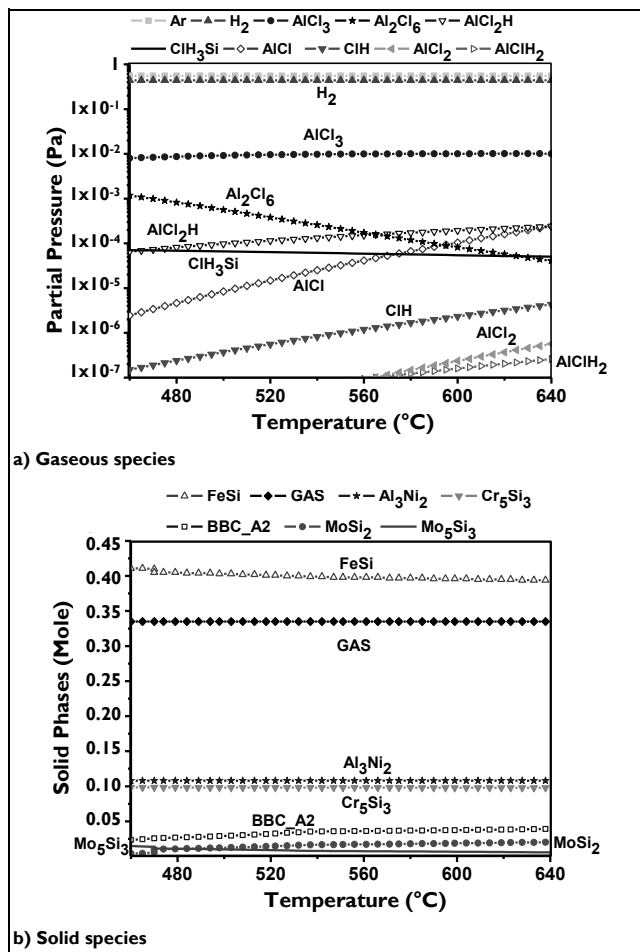


Figure 1. Thermodynamic simulation of aluminum-silicon co-deposition process on the austenitic stainless steels.

The thermodynamic simulations were performed to obtain approximations of the quantity of the Al and Si compounds formed in the CVD-FBR reactor during the deposition process. The input conditions included Al(s), Si(s), substrate and Ar/HCl/H<sub>2</sub> gas mixture. The possible solid phases that could be encountered during the process of co-deposition of aluminum-silicon on the two austenitic stainless steels were also determined as a function of temperature. The simulation was carried out between 460 and 640

$^\circ\text{C}$ , as shown in Figure 1b), where there are solid phases of the co-deposition of the AISI 317 steels were FeSi,  $\text{Al}_3\text{Ni}_2$ ,  $\text{Cr}_5\text{Si}_3$ , BBC\_A2,  $\text{Mo}_5\text{Si}_3$  and  $\text{MoSi}_2$ , where the compound BBC\_A2 is formed by  $\text{Fe}_{0.532}\text{Al}_{0.263}\text{Mn}_{0.193}\text{Cr}_{0.005}\text{Si}_{0.005}$ . The solid-phase simulation for the AISI 304 steel specimen increased the amount of  $\text{Al}_2\text{Fe}$  because this steel had more iron, and the  $\text{Mo}_5\text{Si}_3$  disappeared because the molybdenum content is very low compared to the AISI 317 steel. FeSi is the most stable compound throughout the temperature range investigated, followed by  $\text{Cr}_5\text{Si}_3$  and  $\text{Al}_3\text{Ni}_2$ . The compounds BBC\_A2 and  $\text{Al}_2\text{Fe}$  are in small quantities; it is also shown that when BBC\_A2 increase,  $\text{Al}_2\text{Fe}$  decreases. Analyzing data from the simulation thermodynamics of the gas and solid phases, it is likely that silicon increased in the coating during the co-deposition of aluminum-silicon at temperatures below  $580^\circ\text{C}$ ;  $540^\circ\text{C}$  was selected as a possible test temperature for the co-deposition of aluminum-silicon to investigate the increase in the amount of silicon present in the coating.

Pre-eliminate tests of the co-deposition were conducted in the CVD-FBR reactor using a bed formed by a 5% aluminum powder, 5% silicon powder and 90% inert alumina bed. It was fluidized with 61% argon and by a mixture of 37.1% hydrogen and 1.9% hydrochloric acid as a gas activator for a period of 90 minutes at  $580^\circ\text{C}$ ; these values yielded the best deposition conditions for the aluminum coating. The above conditions yielded good coatings approximately  $12 \pm 4 \mu\text{m}$  thick, but the amount of silicon incorporated into the coating was less than 0.5%. Therefore, the ratio of silicon to aluminum was changed to 9 % silicon and 1 % aluminum; this still only produced aluminum coatings with minimal amounts of silicon. The ratios of the active gases HCl/H<sub>2</sub> were then changed from 1/19 to 1/14; the amounts of aluminum and silicon in the bed were also changed from 5 % to 1 % and from 5 % to 9 %, respectively, to achieve the incorporation of silicon at  $580^\circ\text{C}$ . This was still not successful: only aluminum coatings were obtained. The relationship of HCl/H<sub>2</sub> was also reduced to 1/14 to produce chlorine coatings; the deposition time was also changed to 45 minutes. Unfortunately, these modifications did not produce uniform coatings or increased amounts of silicon in the materials. As the incorporation of silicon was lowest in the co-deposition aluminum-silicon, the deposition temperature was lowered to  $540^\circ\text{C}$  because there was more  $\text{ClH}_3\text{Si}$  at this temperature, which provided a greater possibility of deposited silicon; also, the thermal activation would be improved, likely producing a quality aluminum-silicon coating. It was shown that the coatings vary significantly based on the active gases, amounts of aluminum and silicon in the bed and the deposition time; these parameters greatly affect the co-deposition of aluminum-silicon. The best aluminum-silicon coatings were obtained when the deposition was performed at  $540^\circ\text{C}$  with a ratio of active gases HCl/H<sub>2</sub> of 1/15.3 with 2.5 g of aluminum powder and 7.5 g of silicon powder in the bed and a ratio of 45 % active gases to 55 % neutral gases. The best deposits are reached in the early stages of bed fluidization because the fluid bed has a low gas velocity at this time. Aluminum-silicon co-deposition was achieved under the above parameters; the temperature was then changed to  $520^\circ\text{C}$  and  $560^\circ\text{C}$  because  $580^\circ\text{C}$  did not yield silicon in the coating. The other parameters were kept constant to observe the influence of temperature, but non-homogeneous layers were obtained. This temperature change was shown to affect the co-deposition of aluminum-silicon. For a new co-deposition, the amount of active gases and inert gases H<sub>2</sub>/HCl must be varied; therefore, the influence of temperature was not observable because it created a new deposition with other conditions and most likely another composition. The coatings created at  $540^\circ\text{C}$  with an exposure time of 60 minutes were chosen because they had the best characteristics.

Coatings created at 45 minutes were very thin, and coatings created at 90 minutes were thick; the Gaussian behavior of this deposition method produced a maximum near 60 minutes. The morphologies of the aluminum-silicon coatings were studied to evaluate their characteristics and the effect of heat treatment of these coatings on the two austenitic stainless steels. Figure 2 shows the surface of the aluminum-silicon coating on the two steels, using the technique of backscattered electrons, and the graph of the chemical composition analysis by EDAX. In these images, a slight conical shape of the coating growth can be seen. Figure 2a shows the aluminum-silicon coating on the steel AISI 317, which has an irregular shape in the form of cones with different sizes. The coating has a composition of 62.52% aluminum, 17.6% iron, 7.51% nickel, 6.76% chromium, 4.51% silicon, 0.68% manganese and 0.42% molybdenum. Figure 2b shows the aluminum-silicon coating on the AISI 304 steel. This coating had larger cones and has a more defined conical or pyramidal form. Its composition was 67.88% aluminum, 15.03% iron, 6.21% nickel, 6.76% chromium, 3.59% silicon and 0.33% manganese.

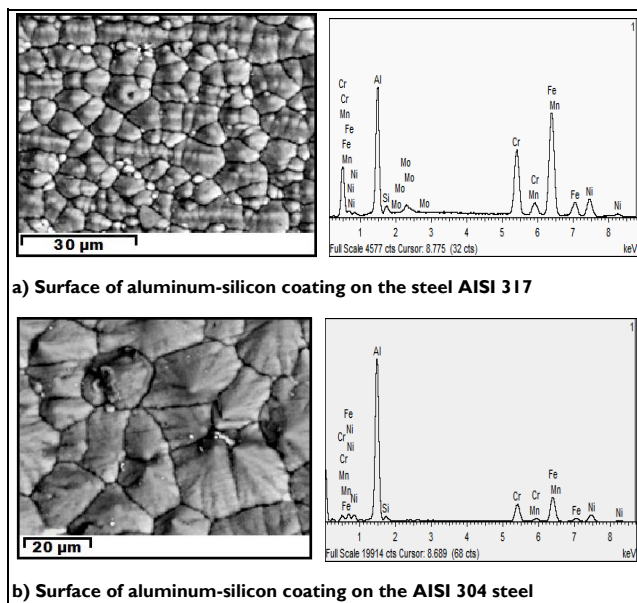


Figure 2. Surface of aluminum-silicon coatings on the stainless steels.

Figure 3 shows the cross section of the aluminum-silicon coating for the two austenitic stainless steels without heat treatment. The aluminum-silicon coatings had a thickness of  $6.5 \mu\text{m}$  ( $\pm 2 \mu\text{m}$ ); these were thinner than the aluminum coating and may be due to the incorporation of silicon in the coating, which reduces the diffusion of aluminum through the  $\text{Fe}_2\text{Al}_3$  layer, slowing the growth of the layer. The line profile of Figure 3a shows that  $\text{Fe}_2\text{Al}_3$  is distributed throughout the coating. This compound is shown in greater proportion in the outer coating and in lesser proportion inside the coating and the substrate-coating interface. There are other compounds that are distributed throughout the coating, including  $\text{Al}_2\text{FeSi}$ ,  $\text{Cr}_3\text{Si}$ ,  $\text{AlCrFe}$  and  $\text{AlFeNi}$ . In Figure 3b, there is a greater diffusion of aluminum into the substrate and of iron into the coating. There is also a decrease in aluminum and a corresponding increase of iron with a slope less steep than for the coating on the steel AISI 317. The aluminum-silicon coating for AISI 317 steel shows approximately 2% each of molybdenum and manganese; these data are not included in the line analysis and thus the graphics do not display correctly. The other elements are more relevant than these. The coating of steel AISI 304 has approximately 1% manganese, but neither was not to overload the figure.

The amounts of aluminum, iron, chromium and nickel in the aluminum-silicon coating on both types of stainless steel have the same behavior as the aluminum coatings on these same steels and follow a similar trend. The silicon in solid solution that is within the crystal lattice of the inter-metallic compounds does not substantially affect its crystalline structure but decrease the growth of the inter-metallic compounds of aluminum. This silicon facilitates the formation of  $\text{Fe}_x\text{Si}_y\text{Al}_z$ , which acts as a diffusion barrier and restricts the growth of the  $\text{Fe}_2\text{Al}_3$  layer (Maitra, & Gupta, 2002; Perez et al., 2006).

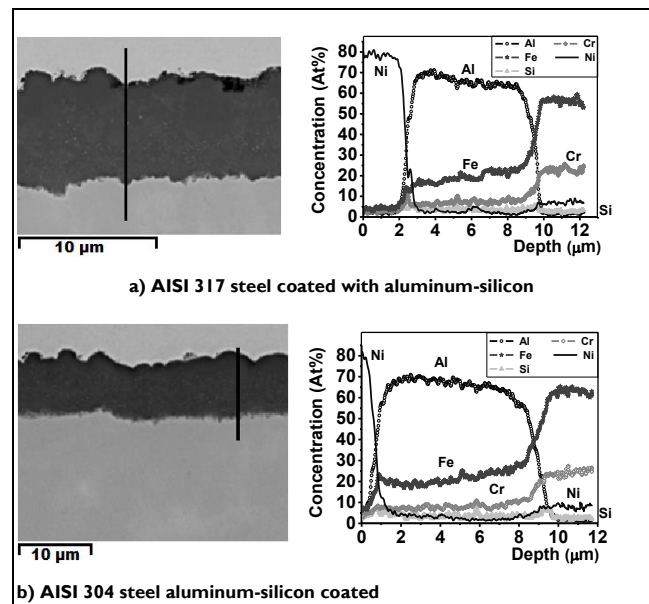


Figure 3. Cross section of the AISI 317 steel and AISI 304 coated with aluminum-silicon without heat treatment.

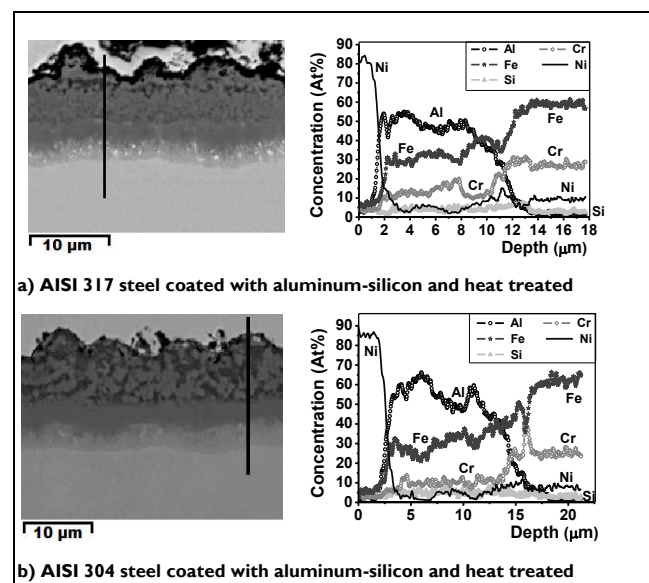


Figure 4. Cross section of the AISI 317 steel and AISI 304 steel coated with aluminum-silicon and heat treated.

The aluminum-silicon coatings were heat-treated to improve their mechanical properties and the oxidation behavior by increasing the diffusion of the alloying elements. Figure 4a shows the cross-section of the heat-treated aluminum-silicon coatings for the two austenitic stainless steels. It is shown that the coating composition varies depending on the thickness. The coating on the AISI 317

steel had three zones: one approximately 5.5  $\mu\text{m}$  thick, composed of  $\text{Al}_2\text{FeSi}$ ,  $\text{Cr}_3\text{Si}$ ,  $\text{AlCrFe}$  and  $\text{AlFeNi}$ , where the  $\text{FeAl}$  is in greater proportion in the outer layer with the darker areas lower in alu-

minium ( $\text{FeAl}$ ) and the gray area lower in aluminum and higher in iron; and lastly a zone rich in nickel that may contain  $\text{AlFeNi}$  and ends with a 2  $\mu\text{m}$  thick zone formed by the diffusion of aluminum. The substrate also appears to have some areas rich in molybdenum.

The heat-treated aluminum-silicon coating on the AISI 304 steel is shown in Figure 4b, which has the same three areas as the AISI 317 steel specimen with the same compounds. In this coating, the outer zone is 9  $\mu\text{m}$  thick, followed by a 2.8  $\mu\text{m}$  thick dark gray zone and ends with a zone 3.2  $\mu\text{m}$  thick that is lighter gray, corresponding to the diffusion of aluminum on the substrate.

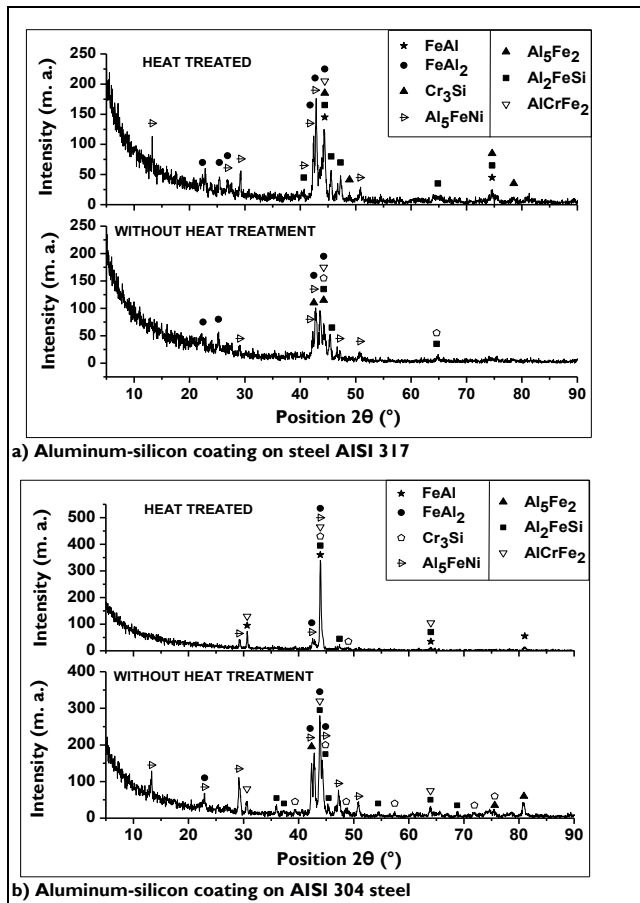


Figure 5. Analysis of X-ray diffraction for the coatings on steel AISI 317 and AISI 304

Figure 5a shows the grazing incidence diffractograms for the AISI 317 steel specimen coated with aluminum-silicon with and without heat treatment. This figure shows that the crystalline structure of the coating without heat treatment is more amorphous than the heat-treated coating. The change of the inter-metallic compounds in the coating without heat treatment is also shown to be  $\text{Al}_5\text{Fe}_2$ ,  $\text{FeAl}_2$ ,  $\text{Al}_2\text{FeSi}$ ,  $\text{Cr}_3\text{Si}$ ,  $\text{AlCrFe}_2$  and  $\text{Al}_5\text{FeNi}$ . After heat treatment,  $\text{Al}_5\text{Fe}_2$  disappears and  $\text{FeAl}$  is formed. The percentage of aluminum decreases in the cross section of the coating while the percentages of iron, chromium and nickel increase so that the phases of these elements become more stable. Figure 5b shows the grazing incidence diffractograms for the AISI 304 steel specimen with the aluminum-silicon coating with and without heat treatment. This figure shows that this coating was less amorphous after heat treatment

and also had a greater transformation of  $\text{Fe}_2\text{Al}_5$  and  $\text{FeAl}_2$  into  $\text{FeAl}$  because the peak of  $\text{FeAl}$  is more pronounced than in the coatings of the other steel, the peaks of  $\text{Fe}_2\text{Al}_5$  disappear and the peaks of  $\text{FeAl}_2$  are few and insignificant. Heat treatment favored transformations to aluminum-rich phases; others transformed to higher contents of iron. Consequently, the mechanical properties and corrosion resistance of the coatings were improved.

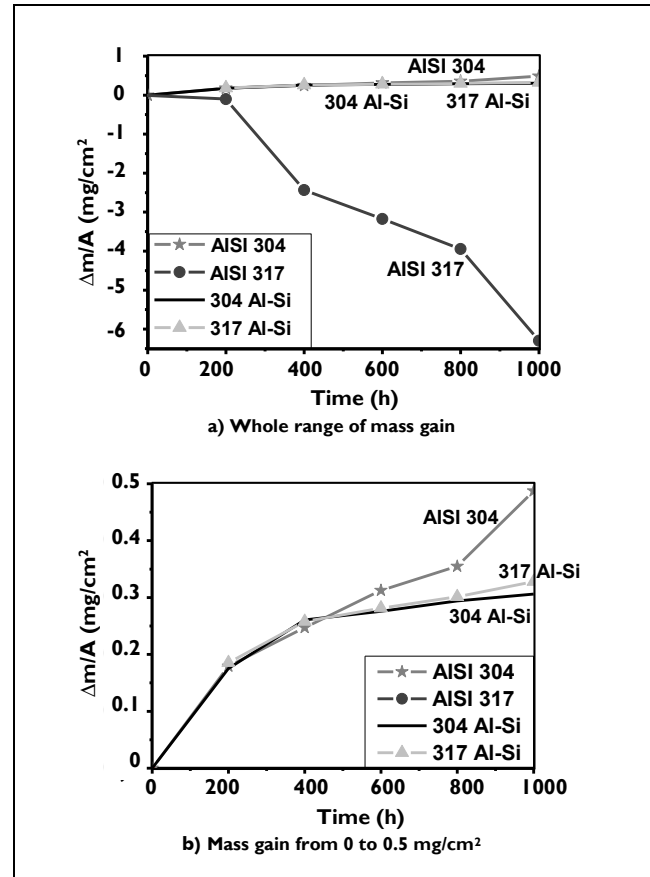


Figure 6. Mass gain of stainless steel with aluminum-silicon coated and uncoated, oxidized in the loop steam at 750 °C

### Steam oxidation

The specimens were exposed to 750 °C in a steam loop to assess the degree of protection provided by these coatings under supercritical temperature and in aggressive environments. Both uncoated substrates behaved differently because the AISI 304 steel performed well and gained little mass, while the AISI 317 steel lost significant weight compared to AISI 304 steel. The coated steels gained little weight during the thousand hours of exposure and are highly resistant to oxidation. When the corrosive attack began, the coated steel gained mass at high speed in the first 400 hours and then more slowly because it has formed a superficial alumina layer with an oxide rich in silicon, chromium and nickel, protecting the coating from additional corrosive attack (Kobayashi, & Yakou, 2002; Huttunen, Kalidakis, Stott, Perez, & Lepistö, 2009). Unlike the uncoated steels, the coated steels showed a linear attack that does not decrease with time. The corrosion rate of the AISI 304 steel specimen tended to increase over time, while the AISI 317 steel specimen experienced high weight loss because the oxide layer that forms in the early hours grows quickly and then slowly, leaving the substrate exposed to corrosive attack. Figure 6 shows the mass gain of the stainless steels coated in aluminum-silicon and uncoated, oxidized in the loop steam at 750 °C.

It can be concluded that the FBCVD process can yield aluminum-silicon coatings 7  $\mu\text{m}$  thick at a deposition temperature of 540 °C and a deposition time of 1 hour. Additionally, after heat treatment, these layers can grow up to 12  $\mu\text{m}$  thick, and a zone of interdiffusion into the substrate appears. The thermodynamic simulation is shown to be a good tool to select the working conditions and understand how the aluminum and silicon halides are affecting the deposition of the aluminum-silicon coating. However the results of the thermodynamic simulation that described the solid species and compounds formed during the deposition were not the same as those that were observed experimentally. The EDX analysis shows that chromium is present in an aluminum-silicon coating. It is reported that during the deposition of aluminum in stainless steels, Cr diffuses readily into the coating to form  $\text{Cr}_5\text{Al}_8$  on the outer surface (Kuo-Liang, Fan-Shiong, & Goa-Shee, 2003); however, the XRD results of this study do not show the formation of this compound.

## Conclusions

\* The FBCVD is an effective technique to obtain very uniform and homogeneous aluminum-silicon coatings on austenitic steels at low temperatures, over short durations and under low atmospheric pressure. Aluminum coatings of more than 8  $\mu\text{m}$  thick can be obtained.

\* The conditions of deposition of aluminum coatings are optimized by CVD-FBR at temperatures below 600 °C that do not affect the microstructure of austenitic stainless steels. Furthermore, the behavior of these coatings in steam oxidation conditions is significantly higher than that observed on uncoated substrates.

\* The CVD-FBR is an important alternative to improve the oxidation resistance in the steam of austenitic stainless steels by the deposition of aluminum coatings at temperatures below 600 °C for short durations and low costs.

\* The aluminum coating as deposited by FBCVD forms intermetallic compounds with the iron present, forming  $\text{Al}_5\text{Fe}_2$ ,  $\text{FeAl}_2$ ,  $\text{Al}_2\text{FeSi}$ ,  $\text{Cr}_3\text{Si}$ ,  $\text{AlCrFe}_2$  and  $\text{Al}_5\text{FeNi}$ . After heat treatment,  $\text{Al}_5\text{Fe}_2$  disappears, and  $\text{FeAl}$  is formed by diffusion, improving oxidation resistance. The coating is extended after heat treatment by the interdiffusion of iron and chromium outward and the aluminum into the substrate, reaching up to 12  $\mu\text{m}$  thick.

\* The aluminum-silicon deposited on the coating forms alumina on the surface and acts as a shield against oxidation. The aluminum-silicon coating is able to extend the life of AISI 304 and 317 stainless steels under steam oxidation at 750 °C by more than 80 times.

## Acknowledgements

Jose Marulanda expresses the authors' gratitude to COLCIENCIAS and UNIVERSIDAD TECNOLÓGICA DE PEREIRA for the doctoral fellowship.

## References

Abella, J. M. (2003). *Láminas delgadas y recubrimientos. Preparación, propiedades y aplicaciones*. Spain: Consejo superior de investigaciones científicas CSIC.

Anastassiou, A., Christoglou, C., & Angelopoulos, G. N. (2010). Formation of aluminide coatings on Ni and austenitic 316 stainless steel by a low temperature FBCVD process. *Surface & Coatings Technology*, 204, 2240–2245.

Brossard, J. M., Hierro, M. P., Sánchez, L., Bolívar, F. J., & Pérez, F. J. (2006). Thermodynamical analysis of Al and Si halide gaseous precursors in CVD. Review and approximation for deposition at moderate temperature in FBR-CVD process. *Surface & Coatings Technology*, 201, 2475–2483.

Chaliampalias, D., Vourlias, G., Pistofidis, N., Pavlidou, E., Stergiou, A., & Stergioudis, G. (2007). Deposition of zinc coatings with fluidized bed technique. *Materials Letters*, 61, 223–226.

Choy, K. L. (2003). Chemical vapour deposition of coatings. *Progress in Materials Science*, 48, 48–57.

Christoglou, Ch., Voudouris, N., & Angelopoulos, G. N. (2002). Formation and modelling of aluminide coatings on iron by a fluidized bed CVD process. *Surface and Coatings Technology*, 155, 51–58.

Christoglou, Ch., Voudouris, N., Angelopoulos, G. N., Pant, M., & Dahl, W. (2004). Deposition of aluminium on magnesium by a CVD process. *Surface and Coatings Technology*, 184, 149–155.

Golman, B., & Shinohara, K. (1999). Comparison of moving bed reactors for chemical vapor deposition coating of fine particles. *Advance powder Technology*, 10, 65–76.

Hao-Tung, L., Sheng-Chang, W., Jow-Lay, H., & Shin-Yun, C. (2007). Processing of hot pressed  $\text{Al}_2\text{O}_3\text{-Cr}_2\text{O}_3/\text{Cr}$ -carbide nanocomposite prepared by MOCVD in fluidized bed. *Journal of the European Ceramic Society*, 27, 4759–4765.

Huttunen, S. E., Kalidakis, S., Stott, F. H., Perez, F. J., & Lepistö, T. (2009). High-temperature erosion-oxidation of uncoated and FB-CVD aluminized and aluminized-siliconized 9Cr–1 Mo steel under fluidized-bed conditions. *Wear*, 267, 2223–2234.

Kim, J., & Young, G. (2006). Effect of agitation on fluidization characteristics of fine particles in a fluidized bed. *Powder Technology*, 166, 113–122.

Kobayashi, S., & Yakou, T. (2002). Control of intermetallic compound layers at interface between steel and aluminum by diffusion-treatment. *Materials science and engineering: A*, 338, 44–53.

Kuo-Liang, W., Fan-Shiong, C., & Goa-Shee, L. (2003). The aluminizing and Al/Si codeposition on AISI HP alloy and the evaluation of their carburizing resistance. *Materials Science and Engineering: A*, 357, 27–38.

Maitra, T., & Gupta, S. P. (2002). Intermetallic compound formation in Fe–Al–Si ternary system: Part II. *Materials Characterization*, 49, 293–311.

Pérez, F. J., Hierro, M. P., Trilleros, J. A., Carpintero, M. C., Sanchez, L., & Bolivar, F. J. (2006). Aluminum and aluminum/silicon coatings on ferritic steels by CVD-FBR technology. *Materials Chemistry and Physics*, 97, 50–58.

Pérez, F. J., Hierro, M. P., Trilleros, J. A., Carpintero, M. C., Sanchez, L., Brossard, J. M., & Bolivar, F. J. (2006). Iron aluminide coatings on ferritic steels by CVD-FBR technology. *Intermetallics*, 14, 811–817.

Pérez, F. J., Pedraza, F., Hierro, M. P., & Hou, P. Y. (2000). Adhesion properties of aluminide coatings deposited via CVD in fluidised bed reactors CVD-FBR on AISI 304 stainless steel. *Surface and Coatings Technology*, 133, 338–343.

Sanchez, L., Bolivar, F. J., Hierro, M. P., & Perez, F. J. (2008). Iron aluminide coatings on ferritic steels by CVD-FBR modified process with Hf. *Intermetallics*, 16, 1161–1166.

Thermocalc Software AB. Version P (2003). Stockholm, Sweden: Fundation of Computational Thermodynamics.

Tsipas, D., Anthimides, K., & Flitris, Y. (2003). Deposition of hard and/or corrosion resistant, single and multielement coatings on ferrous and nonferrous alloys in a fluidized bed reactor. *Journal of materials processing technology*, 134, 145–152.

Zhan, Z., He, Y., Wang, D., & Gao, W. (2006). Low-temperature processing of Fe–Al intermetallic coatings assisted by ball milling. *Intermetallics*, 14, 75–81.